

# Timing with Resonant Gravitational Wave Detectors: an Experimental Test

V. Crivelli Visconti, A. Ortolan, L. Taffarello, G. Vedovato

*INFN, Laboratori Nazionali di Legnaro, via Romea 4, I-35020, Legnaro, Padova, Italy*

M. Cerdonio

*Dipartimento di Fisica, Università di Padova and INFN, Sezione di Padova,*

*via Marzolo, 8 35100 Padova, Italy*

G. A. Prodi and S. Vitale

*Dipartimento di Fisica, Università di Trento and INFN, Gruppo Collegato di Trento,*

*Sezione di Padova, I-38050, Povo, Trento, Italy*

PACS numbers: 4.80; 95.55 Ym

## Abstract

We measure the time of arrival  $t_o$  of a force signal acting on a room temperature gravitational wave detector. The detector has a noise spectral density whose shape is a rescaled replica of that predicted for the two subkelvin detectors located in Italy, once at their sensitivity goal.  $t_o$  is expressed as  $t_o = t_\phi + kT_o$  where  $T_o$  is half the natural period of oscillation of the detector,  $|t_\phi| \leq T_o/2$ , and  $k$  is an integer. We measure the phase part  $t_\phi$  with an accuracy of  $\sigma_{t_\phi} \approx 174 \mu s / SNR$ , where  $SNR$  is the signal to noise ratio for the signal amplitude. We also find that for  $SNR \geq 20$ , the error on  $k$  is  $\delta k \ll 1$  so that the total statistical error on the arrival time reduces to the phase error  $\sigma_{t_\phi}$ . We discuss how this last result can be achieved even for smaller values of  $SNR$ , by better tuning the modes of the detector. We finally discuss the relevance of these results for source location and spurious events rejection with the two subkelvin detectors above.

## 1. Introduction

Two subkelvin ( $T \approx 50 \text{ mK}$ ), resonant ( $\approx 1 \text{ KHz}$ ) gravitational wave detectors aimed at a burst sensitivity of  $h_{\min} \cong 3 \times 10^{-20}$  and a post-detection bandwidth of  $\approx 50 \text{ Hz}$ <sup>1</sup>, have been built in Italy<sup>2</sup> and they are going to operate in coincidence in the near future.

The experiment's target is to detect bursts from supernovae explosions or from coalescence of binary neutron star systems. For this kind of signals the relatively large bandwidth will open the possibility<sup>3</sup> of accurate timing.

Timing information can be used both to locate the source<sup>2</sup>, or at least some of its coordinates, and to veto candidate events that are not compatible with light's speed propagation<sup>4,5</sup>.

In order to demonstrate the practical feasibility of absolute timing with resonant detectors, we have performed an experiment with a room temperature detector connected to our standard data analysis system<sup>6</sup>. The detector is excited by a force pulse generated by a capacitive actuator and the time of arrival of the pulse is measured by looking at the maximum of the output of the Wiener filter.

The detector has a relatively poor sensitivity as compared to cryogenic ones, but its resonant frequencies and its post detection bandwidth happen to be close to those expected for the subkelvin detectors at their sensitivity goal. As the timing accuracy depends only on these parameters, the results obtained with the present room temperature detector can be scaled directly to the subkelvin ones.

The plan of the paper is as follows: in Sect. 2 we briefly describe the properties of signals and noise in g.w. resonant detectors and then, by means of the maximum likelihood approach, we give theoretical predictions for the uncertainties in the estimate of the signal amplitude and time of arrival for a gravitational wave detector. Sect. 3 and 4 are devoted to the description of the experimental apparatus and to the experimental results respectively. Finally in Sect. 5 we discuss the relevance of our results for the existing cryogenic detectors.

## 2. The estimate of the time of arrival

The estimate of the arrival time of a signal in the presence of gaussian noise is a well-established problem in signal analysis<sup>7, 8</sup>. In this section we summarize some results that are relevant for the discussion of a timing experiment with resonant detectors.

The data consist of a series of samples:

$$x_\alpha = \varepsilon_\alpha + A_0 f(t_\alpha - t_0) \quad (-N \leq \alpha \leq N) \quad (1)$$

where  $\varepsilon_\alpha$  is the  $\alpha^{\text{th}}$  sample of a gaussian, time invariant, zero-mean stochastic process and  $f(t-t_0)$  is a signal of unit amplitude arriving at time  $t_0$ .  $A_0$  is the "true" signal amplitude that has to be estimated together with  $t_0$ .

In order to give an estimate for  $A_0$  and  $t_0$ , the method of maximum likelihood<sup>9</sup> searches for the minimum of the log-likelihood function:

$$\Lambda(A, t) = \sum_{\alpha, \beta=-N}^N \mu_{\alpha\beta} [x_\alpha - Af(t_\alpha - t)] \times [x_\beta - Af(t_\beta - t)] \quad (2)$$

as a function of A and t. In eq. 2 the matrix  $\mu_{\alpha\beta}$  is the inverse of the cross correlation matrix  $\langle \varepsilon_\alpha \varepsilon_\beta \rangle = \mu_{\alpha\beta}^{-1}$  where the brackets  $\langle \rangle$  indicate the mean value.

For any given t the minimum of  $\Lambda(A,t)$  is readily found at

$$\hat{A}(t) = \frac{\sum_{\alpha, \beta=-N}^N \mu_{\alpha\beta} x_\alpha f(t_\beta - t)}{\sum_{\alpha, \beta=-N}^N \mu_{\alpha\beta} f(t_\alpha - t) f(t_\beta - t)} \quad (3)$$

with an error

$$\sigma_{\hat{A}}^2(t) = \frac{1}{\sum_{\alpha, \beta=-N}^N \mu_{\alpha\beta} f(t_\alpha - t) f(t_\beta - t)} \quad (4)$$

We assume from now on that, as usually happens in practice, the data span a long enough time interval so that the error in eq. (4) is in practice independent of t:  $\sigma_{\hat{A}}^2(t) = \sigma_{\hat{A}}^2(t_o) = \sigma_A^2$ .

Eqs. (3) and (4) are fully equivalent to the results of the Wiener filter method and  $\hat{A}(t)$  can then be considered as the output of this filter as well.

The minimum of  $\Lambda(A,t)$ , at  $A = \hat{A}(t)$ , is given by:

$$\Lambda(t) = \sum_{\alpha, \beta=-N}^N \mu_{\alpha\beta} x_\alpha x_\beta - \frac{\hat{A}^2(t)}{\sigma_A^2} \quad (5)$$

Eq. (5) shows that the best estimate for the arrival time t, is the value that maximize the signal to noise ratio  $SNR(t) = \left| \frac{\hat{A}(t)}{\sigma_A} \right|$ .

By substituting eq. (1) in eq. (3), and by shifting the time axis until  $t_o=0$ , one gets that

$\hat{A}(t)$  can be written as  $\hat{A}(t) = A_o R(t) + A_r(t)$ , where R(t) is given by

$$R(t) = \frac{\sum_{i, k=-N}^N \mu_{\alpha\beta} f(t_\alpha - t) f(t_\beta)}{\sum_{i, k=-N}^N \mu_{\alpha\beta} f(t_\alpha) f(t_\beta)} \quad (6)$$

$A_r(t)$  is a zero mean random process that in the limit where  $N \rightarrow \infty$  becomes also time invariant with autocorrelation  $\langle A_r(t) A_r(t + \tau) \rangle = \sigma_A^2 \times R(\tau)$ .

Up to linear terms in the inverse of the “true” signal to noise ratio  $SNR_o = A_o / \sigma_A$ ,  $SNR^2$  can then be expanded as  $SNR^2(t) \approx SNR_o^2 \times \{R^2(t) + 2R(t)[A_r(t)/A_o]\}$ .

For resonant detectors R(t) is the superposition of few exponentially damped oscillating functions with closeby frequencies (Fig. 1). As a consequence R(t) shows a series of maxima and minima approximately spaced by  $T_o/2$ , where  $1/T_o$  is the natural frequency of the detector. The first of these extrema is always located at  $t=0$ .

For high enough values of  $\text{SNR}_o$ , at each maximum of  $R^2(t)$  corresponds a maximum of  $\text{SNR}^2(t)$ . Due to fluctuations, however, the two maxima are not located at the same time value. In the vicinity of the  $\alpha^{\text{th}}$  maximum of  $R^2(t)$ , attained at time  $t=t_k$ ,  $\text{SNR}^2(t)$  can be expanded in powers of  $t_\phi=t-t_k$  and has a maximum, as a function of  $t_\phi$ , at:

$$t_{\phi k} = -\frac{\dot{A}_r(t_k)}{A_o \ddot{R}(t_k)} \quad (7)$$

where  $\dot{A}_r(t_k)$  stands for the time derivative of the random process  $A_r(t)$  evaluated at  $t=t_k$ , and  $\ddot{R}(t_k)$  is the second time derivative of  $R(t)$  at same time. From standard theory of random variables and processes one gets that:

$$\langle t_{\phi k} \rangle = -\frac{d\langle A_r(t_k) \rangle / dt}{A_o \ddot{R}(t_k)} = 0 \quad (8a)$$

$$\langle A_r(t_k) t_{\phi k} \rangle = -\frac{\langle \dot{A}_r(t_k) A_r(t_k) \rangle}{A_o \ddot{R}(t_k)} = \frac{\dot{R}(0)}{A_o \ddot{R}(t_k)} = 0 \quad (8b)$$

$$\langle t_{\phi k}^2 \rangle = \frac{\langle \dot{A}_r(t_k) \dot{A}_r(t_k) \rangle}{A_o^2 \ddot{R}^2(t_k)} = -\frac{\sigma_A^2 \ddot{R}(0)}{A_o^2 \ddot{R}^2(t_k)} \approx \frac{T_o^2}{\text{SNR}_o^2 4\pi^2 |R(t_k)|} \quad (8c)$$

Eqs. (8a) and (8b) state that, within the present approximation,  $t_{\phi k}$  is a zero mean, gaussian variable *independent of*  $A_r(t_k)$ .

Eq. (8c), where the final approximate term has been obtained by using  $\ddot{R}(t_k) \approx (T_o/2\pi)^2 R(t_k)$  and  $R(0)=1$ , shows that the width  $\sigma_{t_{\phi k}} = \sqrt{\langle t_{\phi k}^2 \rangle}$  of the gaussian distribution of  $t_{\phi k}$  is much smaller than the spacing  $T_o/2$  between two adjoining maxima and is:

$$\sigma_{t_{\phi k}} = \frac{T_o}{2\pi \cdot \text{SNR}_k} \quad (9)$$

with  $\text{SNR}_k=R(t_k)\text{SNR}_o$  the signal to noise ratio on the  $\kappa^{\text{th}}$  maximum. Eq. (9) is the classical formula<sup>9</sup> for the “phase” timing of narrowband signals. With this we mean that if the above timing error is converted to a phase error  $\sigma_\phi = \frac{2\pi}{T_o} \sigma_{t_{\phi k}}$ , this amounts to  $\sigma_{\phi k}=1/\text{SNR}_k$ .

Up to this point then, the maximum likelihood criterium gives a discrete series of possible arrival time values  $t_k+t_{\phi k}$ , spaced roughly by  $T_o/2$ . For each of this possible arrival times, the estimate of the amplitude  $\hat{A}(t_k)$  is a gaussian random variable with mean value  $A_o R(t_k)$  and standard deviation  $\sigma_A$ . In order to get a well defined arrival time one has then to pick up the the value  $t^*$  at which  $|\hat{A}(t_k)|$  attains its maximum.

As already stated, for resonant detectors  $R(t)$  can be written as  $R(t)=a(t)\cos(\omega_o t)+b(t)\sin(\omega_o t)$ , with  $\omega_o$  some center “carrier” angular frequency not

more than a few percent far from the detector resonant angular frequency  $2\pi/T_0$ .  $a(t)$  and  $b(t)$  are two slowly varying function of time that consist of a combination of exponentials and beating notes among the various modes of the detector-transducer-amplifier chain. As a consequence  $R(t_k)$ , that attains his maximum at  $t_k=0$  (that we assume to correspond to  $k=0$ ) and that is an even function of  $k$ , can be expanded, for the first few values of  $k$ , as:

$$R(t_k) \approx (-1)^k \cdot (1 - |t_k|/\tau - \omega_*^2 t_k^2 / 2) \quad (10)$$

with  $\tau$  and  $\omega_*$  two constants that obey to  $1/\tau, \omega_* \ll \omega_0$ .

In addition, as for large signal to noise ratios and for  $\alpha$  not too large  $A_r(t_k) \ll A_o |R(t_k)|$ , then  $|\hat{A}(t_k)| = |A_o R(t_k) + A_r(t_k)| \approx A_o |R(t_k)| + (-1)^k A_r(t_k) \equiv A_o |R(t_k)| + A_r^*(t_k)$ . It is easy to calculate that the series  $A_r^*(t_k)$  has autocorrelation  $\langle A_r^*(t_k) A_r^*(t_m) \rangle = \sigma_A^2 |R(t_k - t_m)|$ .

The series  $|\hat{A}(t_k)|$  can then be considered as made of the samples of the “signal”  $A_o |R(t_k)|$  buried into the gaussian zero mean noise  $A_r^*(t_k)$  and all the machinery we have applied then to extract  $t_\phi$  can in principle be applied again to evaluate  $t^*$ .

If this is made, it is straightforward to calculate that the analogous of the function  $R(t)$  in eq. (6) becomes  $R^*(t) \approx (1 - |t|/\tau - \omega_*^2 t^2 / 2)$  and two limiting case are given where quite different results are obtained.

If for all values of  $k$  in eq. (10)  $|t_k|/\tau$  is negligible in comparison to  $\omega_*^2 t_k^2 / 2$ , i.e. if  $\omega_*^2 T_0 \tau / 4 \gg 1$ , then  $R^*(t) = 1 - \omega_*^2 t^2 / 2$  has a well defined second derivative at  $t=0$  and one gets that:

$$\sigma_{t^*} = \frac{1}{\omega_* \cdot SNR_o} \quad (11)$$

In the opposite limit where  $\omega_*^2 T_0 \tau / 4 \ll 1$  instead, the signal  $1 - |t|/\tau$  has an infinite second derivative at the origin and the linear expansion used to get eq. (7) or eq. (11) cannot be used anymore. To estimate  $\sigma_{t_\beta}$  in this case one can use the following argument:  $|\hat{A}(t_k)|$  is approximately a Markov series. Then  $|\hat{A}(t_k)| = |\hat{A}(0)| \cdot (1 - |t_k|/\tau) + \varepsilon \cdot \sigma_A \cdot \sqrt{2|t_k|/\tau}$  where  $\varepsilon$  is a zero mean gaussian variable with unit variance independent of  $|\hat{A}(0)|$ . The probability then that  $|\hat{A}(t_k)| \geq |\hat{A}(0)|$  is the same as the probability that  $\varepsilon \geq SNR_o \sqrt{|t_k|/2\tau}$ . The probability that  $|\hat{A}(t_k)| \geq |\hat{A}(0)|$  and/or  $|\hat{A}(t_{-k})| \geq |\hat{A}(0)|$  is approximately twice as much i.e. the same as the probability that  $|\varepsilon| \geq SNR_o \sqrt{|t_k|/2\tau}$ . In summary this crude reasoning brings to the result that  $t^*$  is approximately  $\chi^2$  distributed with one degree of freedom, with standard deviation

$$\sigma_{i^*} = \frac{2\tau}{SNR_o^2} \quad (12)$$

a result that can be found, based on a more rigorous ground, in ref. 8.

As already stated the times  $t_k$  are, within a few percent, spaced by  $T_o/2$ , i.e.  $t_k = kT_o/2$ . The random variable  $k$  has then a standard deviation

$$\sigma_k = \begin{cases} \frac{\omega_o}{\pi \omega_* SNR_o} \left( \frac{\omega_o}{\omega_*} \right)^2 \ll \frac{\pi}{2} \tau \omega_o \\ \frac{2\omega_o \tau}{\pi SNR_o^2} \left( \frac{\omega_o}{\omega_*} \right)^2 \gg \frac{\pi}{2} \tau \omega_o \end{cases} \quad (13)$$

and when  $\sigma_k \ll 1$  the timing error reduces to the phase contribution only in eq. (9).

In summary the time of arrival  $t$  is expected to be a zero mean random variable with an approximate distribution made of a series of gaussian peaks with gaussian distributed relative amplitudes:

$$F(t) \approx \sum_{m=-\infty}^{\infty} \frac{\omega_o SNR_m}{2\pi \sigma_k} e^{-\frac{[\omega_o SNR_m (t - mT/2)]^2 + (m/\sigma_k)^2}{2}} \quad (14)$$

where the approximation<sup>10</sup> has better accuracy toward low absolute values of  $k$ .

### 3. Experimental Apparatus and Measurement Methods

To experimentally test the above ideas, we have used a room temperature replica of the subkelvin AURIGA detector. The sensitive part of the apparatus is a 2.3 tons cylinder, made of 5056 aluminium alloy, suspended to a single copper wire (see Fig. 2). The fundamental mode of the detector is at  $\approx 850$  Hz. A multiple stage vibration attenuator provides, at this frequency, an attenuation of about 150 dB, which is enough to suppress the environmental noise below the thermal vibrations of the fundamental mode of the bar. The read out consists of an electromechanical capacitive, high mass transducer<sup>2</sup> and a very low noise FET preamplifier<sup>11</sup>.

Briefly the transducer consists of an aluminium disk rigidly connected to one of the bar end-faces. The disk forms the first plate of a capacitor the second plate of which is another disk parallel and very close to the first one ( $\approx 100 \mu\text{m}$ ). This last disk is mechanically connected to the bar by just a thin axial rod, and can thus vibrate in its first, "mushroom" shaped, symmetrical mode. As this mode is coupled to the oscillations of the bar, these modulate the transducer capacitance. The capacitor is charged to a charge of about 1.6  $\mu\text{C}$  by means of a voltage generator which is then disconnected. The capacitance oscillation results then in a voltage signal across the capacitor.

The signal is fed to an FET preamplifier with a  $12.5 \pm 0.1 \text{ G}\Omega$  input impedance and measured noise temperature and resistance of  $T_n \cong 100 \text{ mK}$  and  $R_n \cong 2.4 \text{ M}\Omega$  respectively<sup>11</sup>. The signal is further amplified by a commercial low noise amplifier<sup>12</sup>.

The measurements consist of the following procedure: the bar is excited by a very short pulse of force with known amplitude and time of arrival. The resulting output signal is then collected and analysed in order to estimate, via a suitable processing algorithm, the

amplitude and time of arrival. The true and the estimated values for both parameters are then compared in order to evaluate the measurement errors.

To apply the force pulse, a force actuator is mounted on the opposite side of the bar. This device is just like the transducer except that its first symmetrical mode is found at  $\approx 2800$  Hz, well above the resonant frequency of the detector, and that the capacitor gap is wider ( $200\mu\text{m}$ ) than that of the transducer. The force pulse is generated by feeding on top of the

dc bias, via a decoupling capacitor, a voltage signal  $V(t) = V_o e^{-\frac{t^2}{\tau_o^2}} \cos(\omega_o t)$ , with  $\omega_o \approx 2\pi$  kHz and  $\tau_o \approx 1$  ms from a programmable signal generator. The resulting force pulse

$f(t) = \frac{E_o}{C} V(t)$  thus crudely simulates the shape of the signal expected from a gravitational collapse event.

The signal generator is triggered by an external TTL signal (Fig. 3) which is also sent to a GPS clock that returns the Universal Time (UT) to the acquisition workstation up to a precision of a few hundreds of ns. In this way we are able to tag each impulsive signal with comparable accuracy.

The amplified analog signal is then sampled at 4.9 kHz and converted into an 18 effective bit digital signal which is stored on 4.5 Gbytes magnetic tapes. Because of the presence of analog and digital filters on the acquisition line, a delay is introduced, which has been measured to be  $1.976 \pm 0.001$  ms .

The pulse arrival time is estimated by filtering data as discussed in section 2. Moreover, to keep track of detector parameters drifts due to slow changes of temperature and bias electric field, the Wiener filter has been made adaptive: the filter parameters (zeroes and poles of the transfer function) are periodically adjusted by maximising the signal to noise ratio of a high amplitude calibration pulse. When the maximum SNR is reached, the filter gives the correct amplitude and arrival time of any impulsive event.

For each SNR value we have collected at least a few hundreds of events. At low SNR (i.e.  $\text{SNR} \approx 6$ ), when measured arrival time are spread over many peaks ( $\geq 10$ ), we have collected more than 5000 events.

#### 4. Timing Results

With reference to fig.1, we have separated the uncertainty in the estimate of the arrival time into the "phase error"  $t_{\phi_k}$  and the "peak error"  $k$  by writing  $\hat{t} = t_{\phi_k} + kT_*$  where  $k$  is the nearest integral value to the ratio  $\hat{t}/T_*$ . There is no ambiguity in assigning an event to the corresponding peak order, since peaks are well separated from each other

In Fig 4 we show the joint histogram for  $\phi_k$  and  $k$  for  $\text{SNR}=6$ . We find that within the statistical uncertainty there is no correlation between the mean and variance of  $t_{\phi_k}$  and  $k$  at least for  $k \leq 10$ .

In fig.5 we report the standard deviation of  $t_{\phi_k}$  for events in the central peak ( $k=0$ ) at different SNR. The solid line represents the fit to the experimental data of the power law  $P/\text{SNR}$ , from which we obtain  $P = 178 \pm 3 \mu\text{s}$ . This value has to be compared with  $1/\omega_0$   $185 \mu\text{s}$ .

In Fig. 6 we report the histogram of the distribution of  $k$ , which is just the projection of the bidimensional histogram of Fig. 4 over the  $k$  axis. Again that data refer to  $SNR = 6$ .

In Fig. 7 we plot the standard deviation  $\sigma_k$  of  $k$  as a function of SNR. The error bar associated with each data point of Fig. 7 has been estimated as follows: for  $SNR \leq 10$ ,  $k$  is spread over many integer values and the standard gaussian estimator of the variance is a reasonable choice. In this case the variance of the estimate has a relative error  $\approx \sqrt{(2/N_e)}$ , where  $N_e$  is the total number of events in the histogram.

At high SNR ( $> 10$ ), most of the events fall into the central peak, which gives no contribution to the estimate of the variance, and hence the error on the latter must be much higher than the gaussian estimate. Assuming the Poisson distribution for the rare events falling outside the central peak we calculate that the relative error on  $\sigma_k$  is of order  $1/\sqrt{N_e - N_{e0}}$ , where  $N_{e0}$  is the number of events with  $k = 0$ .

## 5. Conclusions

The experimental results obtained above support quantitatively the standard theory presented in Sec. 1. To be specific the result show that: i)  $t_{\phi_k}$  is independent of  $k$ ; ii) that eq. (9) for the phase noise is obeyed; iii) that, for the kind of “one beatnote” autocorrelation function we achieved with our room temperature detector, eq. 13 holds. It must be noted that the room temperature detector parameters were found<sup>13</sup> to be  $\omega_* \approx 126$  rad/s and  $\tau \approx 75$  ms, so that one is in the régime of equation (13 a), i.e.  $\omega_*^2 T_0 k \tau / 4 > 1$ , only for  $k \geq 3$ . However it can be seen from fig. 7 that experimental data fit the theoretical behaviour of  $\sigma_k$  vs SNR even at high SNR, where events with  $k \geq 3$  are very unlikely. In this sense we say that eq. (13 a) holds.

The overall timing ability of the room temperature detector is then such that for  $SNR > 20$  the total uncertainty on the arrival time is  $\sigma_t \approx 174 \mu\text{s}/SNR$ .

The uncertainty is mainly dominated by the detector being in the régime of eq. (13 a) due to a non optimal matching of the transducer to the detector and to a comparatively poor performance of our FET amplifier as compared, for instance, to a SQUID one.

The transducer used in the present experiment has been indeed optimised to work at low temperature with a low noise SQUID amplifier. Matching to those conditions yielded to a mass of  $M=2.17$  kg and to an unperturbed frequency value for the transducer of  $\nu=875$  Hz at room temperature. An optimal choice for the room temperature detector would have yielded a much lower value for the mass,  $M \approx 0.05$  kg. This detuning is the source of the above mentioned limitation.

When the same transducer will be assembled on AURIGA and if a SQUID noise performance corresponding to a noise energy density per unit frequency of  $\varepsilon \approx 100 \hbar$ , the detector will be found in the régime described by eq. (13 b) with  $\tau \approx 20$  ms. This should give the same timing performance as that achieved above but for  $SNR > 8$ .

We believe that the main result of our test are the prospects it opens for the near future, when different kinds of detectors will be operating together. For the class of impulsive gravitational signals (SN explosions, to give an example) without a characteristic waveform pattern, comparison between different detectors is the only way to reject spurious events

and gain informations on the signal, and accurate timing on each of them is the conditio sine qua non.

At the moment 5 resonant bars are operating worldwide, so that simple triangulations can be performed to determine the source position by measuring time-of-flight delays between different detectors. The timing precision we have reached is sufficient to apply this method even at regional scales, as for the Italian gravitational wave detectors AURIGA, NAUTILUS and VIRGO.

High precision absolute timing, however, opens the way to a more accurate method of analysis of gravitational signals. In fact, it has been shown<sup>2</sup> that with at least 6 resonant bars one can reconstruct on the same wavefront the amplitude and direction of propagation of the wave, in order to solve “the inverse problem” and test the Riemann tensor’s transversality and tracelessness. Source position can also be determined within few arcmin. This method can be easily extended to the upcoming global network of bars (AURIGA, NAUTILUS) and interferometers (TAMA 300, GEO 600, LIGO, VIRGO), which all are expected to have the same sensitivity at 1 kHz, and will thus provide the first actual gravitational wave observatory.

In addition, correlation between instruments operating on different physical principles, like resonant bars and interferometers, is very important not only because it provides a way to compare independently generated data, but also because different detectors have different noise sources and hence spuria rejection will be much more reliable.

<sup>1</sup>M.Cerdonio, P.Falferi, G.A.Prodi, A.Ortolan, S.Vitale and J.P.Zendri, *Physica B* **194** 3 (1994); M. Cerdonio G.A.Prodi, A.Ortolan, S.Vitale and J.P.Zendri, *Nucl. Phys. B*, (Proc. Suppl.) **35**, 75 (1994).

<sup>2</sup>AURIGA at Legnaro INFN National Laboratories, see M. Cerdonio et al., in Proc. of the First Edoardo Amaldi Conference on Gravitational Wave Experiments, E. Coccia, G. Pizzella e F. Ronga Eds (World Scientific - Singapore -1995), p. 176, and Nautilus at Frascati INFN National Laboratories, see P. Astone et al., in Proc. of the First Edoardo Amaldi Conference on Gravitational Wave Experiments, E. Coccia, G. Pizzella e F. Ronga Eds (World Scientific - Singapore -1995), p. 161.

<sup>3</sup>M. Cerdonio, P. Fortini, G.A. Prodi, A. Ortolan and S. Vitale, *Phys. Rev. Lett.* **71** 4107 (1993).

<sup>4</sup> S. Vitale *et al.*, to appear in Proc of the International Conference on Gravitational Waves: Sources and Detectors, Cascina (PI), Italy (1996).

<sup>5</sup>A. Ortolan, PhD Thesis (1992) University of Ferrara; M. Cerdonio, P. Fortini, A. Ortolan and S. Vitale, in Proc. of the 10th Italian Conference on General Relativity and Gravitational Physics; M. Cerdonio, R. D'Auria, M. Francaviglia e G. Magnano Eds., (World Scientific - Singapore -1994), p. 111.

<sup>6</sup> A. Ortolan, G. Vedovato, M. Cerdonio and S. Vitale, *Phys. Rev D***50** 4737 (1994). S. Vitale et al. in Proc. of the First Edoardo Amaldi Conference on Gravitational Wave Experiments, E. Coccia, G. Pizzella e F. Ronga Eds (World Scientific - Singapore -1995), p.

<sup>7</sup> J. A. Lobo, *Mon. Not. R. Astr. Soc.*, **247** (1990) 573-583

<sup>8</sup> P. Swerling, *J. Soc. Indust. Appl. Math.* **7** 152 (1959) and references therein.

<sup>9</sup> see for instance: C.W. Helstrom, "*Statistical Theory of Signal Detection*", (Pergamon, Oxford UK 1968).

<sup>10</sup> F(t) is even normalized in an approximated way.

<sup>11</sup> D. Carlesso, Thesis (1996) University of Padua.

<sup>12</sup> Stanford Research SR560 FET amplifier.

<sup>13</sup> V. Crivelli Visconti, Thesis (1996), University of Rome "la Sapienza"

## Caption to figures

**Fig. 1** Pattern of the autocorrelation function  $R(t)$ , with  $\omega_* = 5300 \text{ rad} / \text{s}$ ,  $Q_* = 200$  and  $\beta = 150 \text{ rad} / \text{s}$ . These parameters has been measured on the room temperature detector.

**Fig. 2** Suspension stages of the room temperature detector. The copper rod wrapped around the bar central section gives a mechanical attenuation of -60 dB at the bar resonant frequency (about 850 Hz) while the overall measured attenuation (metalgummy + lead blocks + steel cantilever + copper rod), at the same frequency, is of the order of -150 dB.

**Fig. 3** Scheme of the excitation and readout systems for timing measurements. The TTL triggering signal is sent both to the syntetized function generator, which excites the bar trough the calibration transducer and to the GPS clock, which provides the time tag associate with the event. The amplified signal from the resonant capacitive transducer is digitized by the ADC and its samples are tagged by the same GPS clock with an accuracy of about  $0.1 \mu\text{s}$ .

**Fig. 4** Complete “peak” vs. “phase” distribution of arrival times with  $SNR = 6$  and over 5000 trials; the "true" arrival time is  $t=0$ . The phase error is given in unit of fraction of the period  $T_0=178 \mu\text{s}$ . Notice that the phase error never exceed  $T_0/4$ .

**Fig. 5** Fit to the experimental data (continuous line—) and theoretical (dotted line ...) curve of the “phase” standard deviation  $\sigma_\phi$  as a function of SNR. The experimental points refer to the central peak events.

**Fig. 6** “Peak” distribution of the arrival times obtained with  $SNR = 6$

**Fig. 7** Experimental ( $\bullet$ ) and theoretical ( $\circ$ ) values of the “peak” error as a function of SNR. If  $\sigma_k \leq 1$  (i.e.  $SNR > 20$ ) the total uncertainty of the arrival time reduces to the phase contribution of Fig. 4.

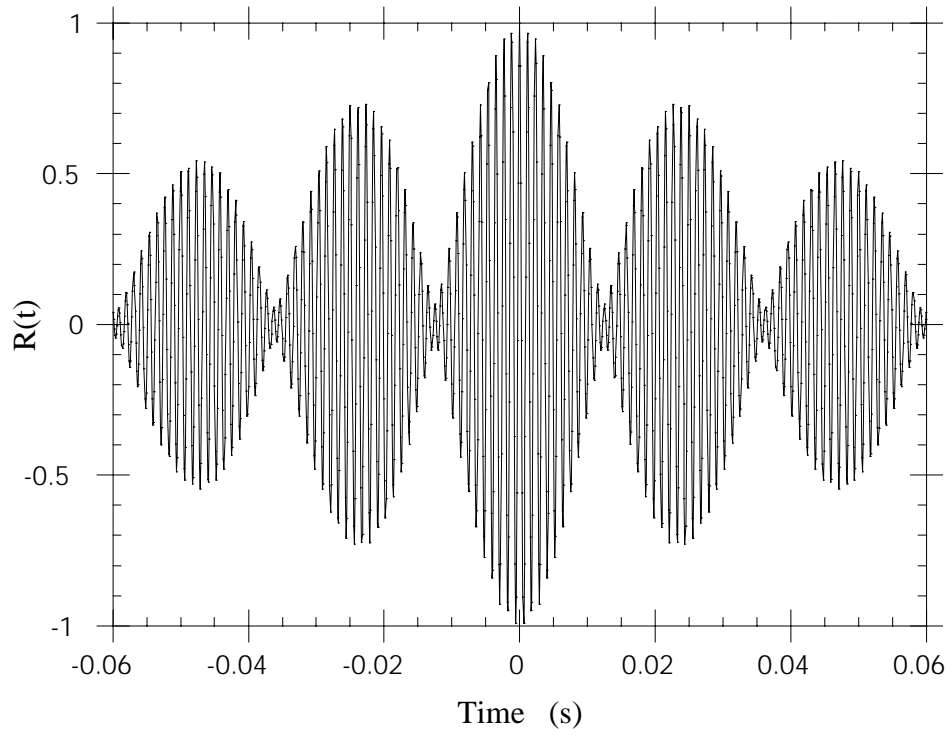


**Fig. 1**

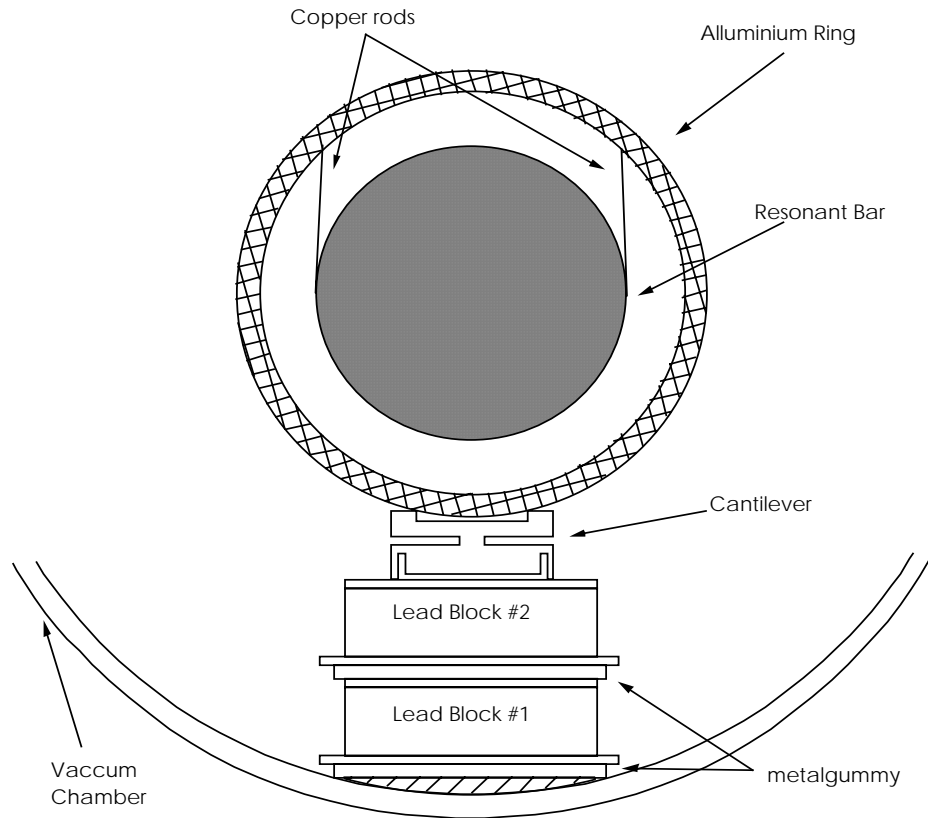


**Fig. 2**

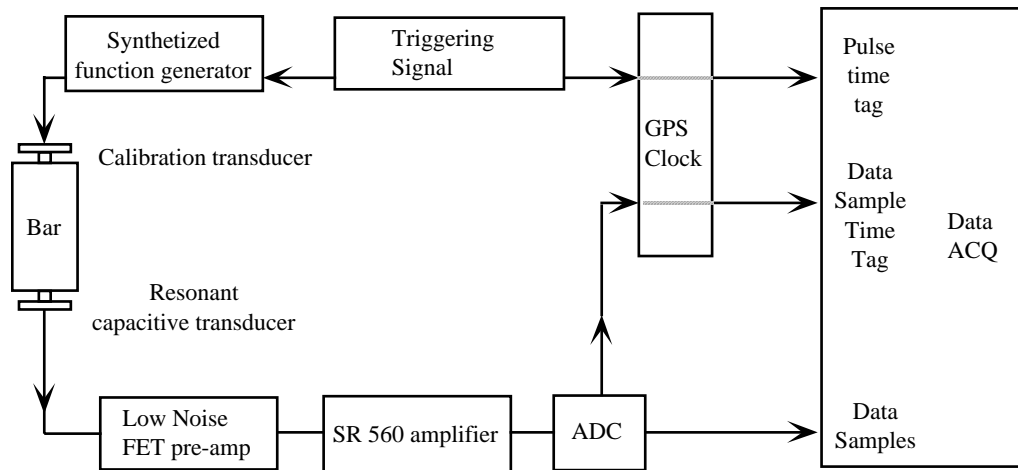


**Fig. 3**

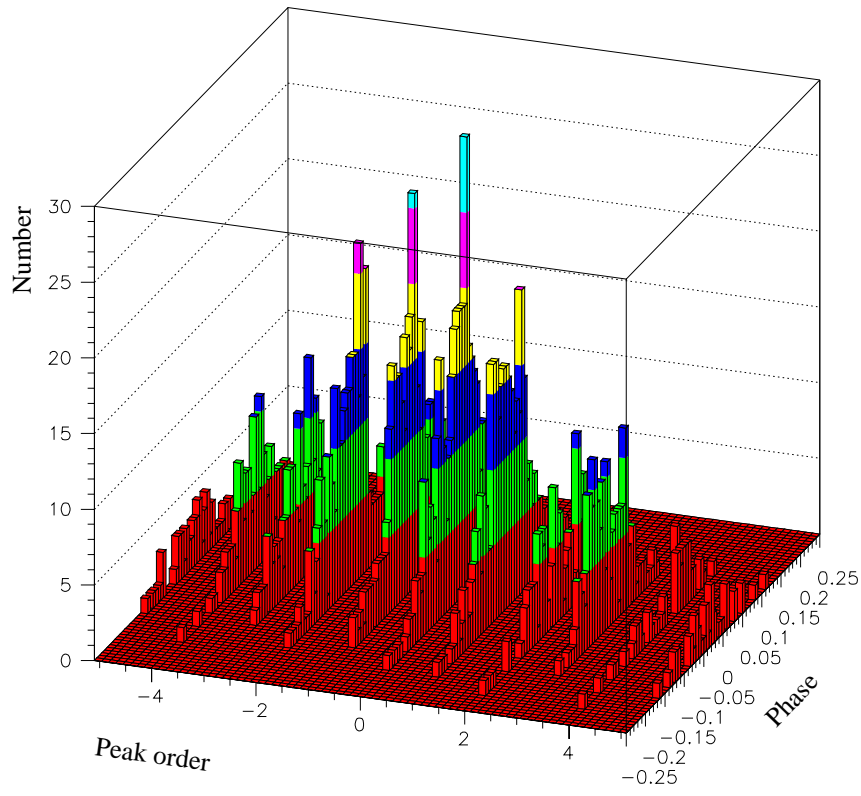


**Fig. 4**

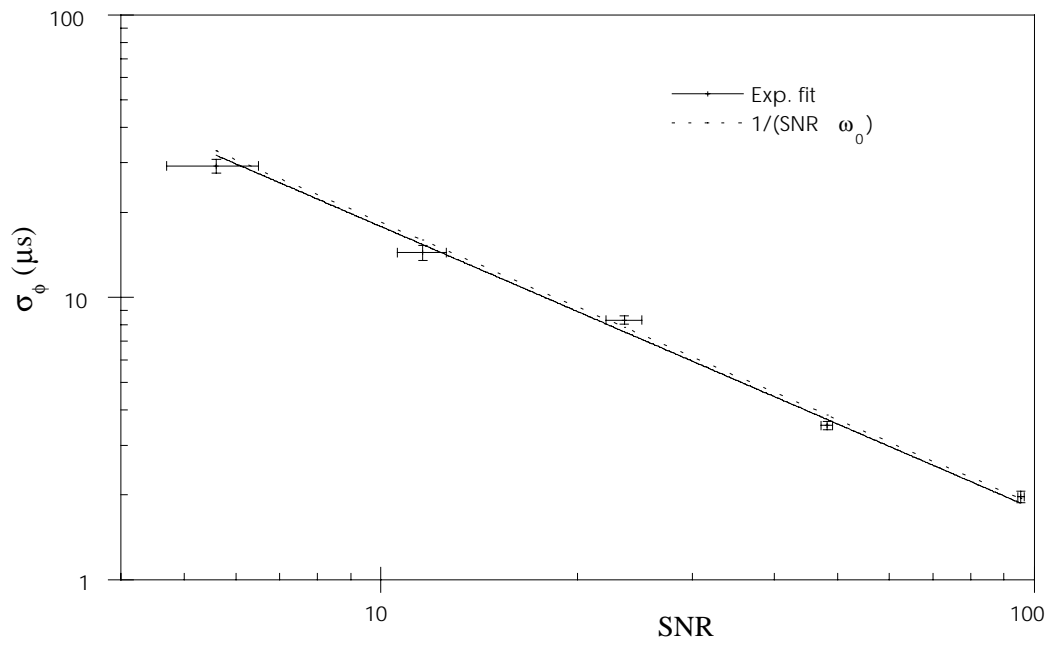


**Fig. 5**

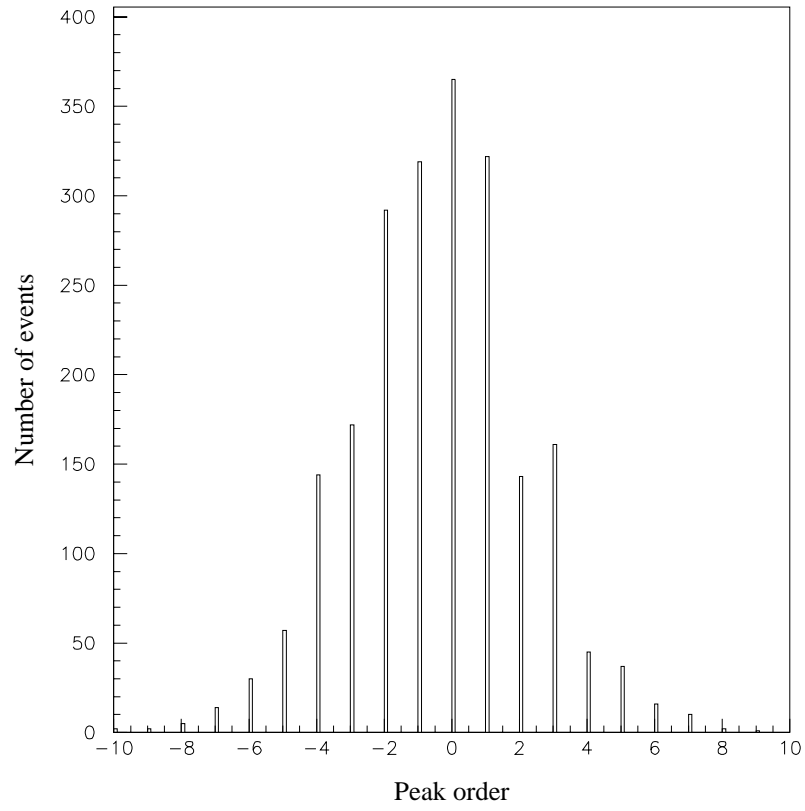


**Fig. 6**

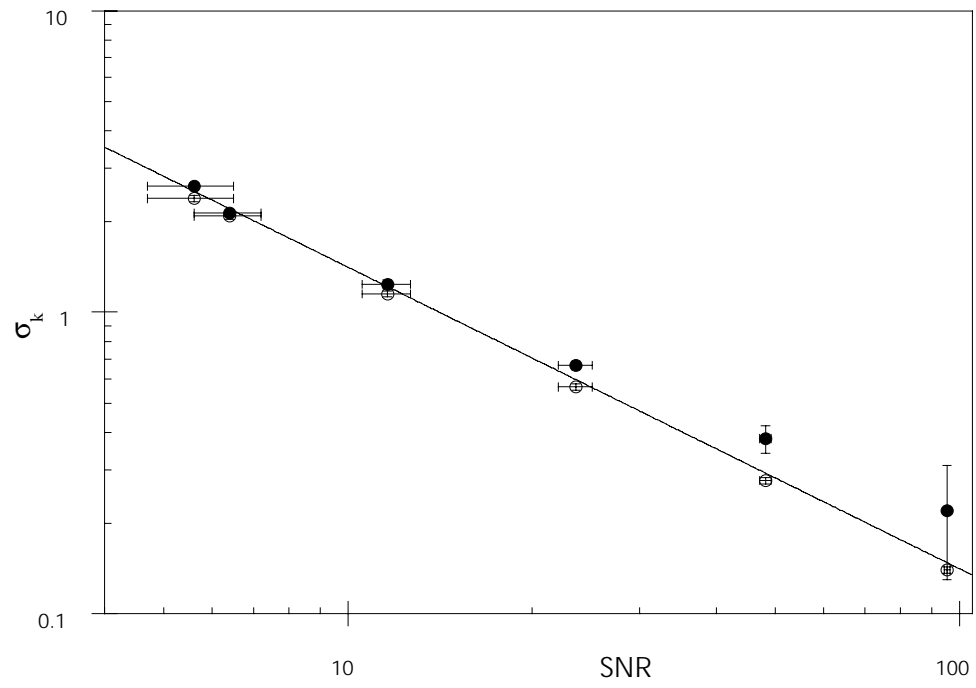


**Fig. 7**